Journal of Applied and Natural Science
15(3), 1051 - 1060 (2023)
ISSN : 0974-9411 (Print), 2231-5209 (Online)
journals.ansfoundation.org

Research Article

Monitoring forest gain and loss based on LandTrendr algorithm and Landsat images in KTH Pati social forestry area, Indonesia

Deha Agus Umarhadi
Department of Forest Management, Faculty of Forestry, Universitas Gadjah Mada, Yogyakarta, Indonesia
Wahyu Wardhana*
Department of Forest Management, Faculty of Forestry, Universitas Gadjah Mada, Yogyakarta, Indonesia
Senawi
Department of Forest Management, Faculty of Forestry, Universitas Gadjah Mada, Yogyakarta, Indonesia
Emma Soraya
Department of Forest Management, Faculty of Forestry, Universitas Gadjah Mada, Yogyakarta, Indonesia

*Corresponding author. E-mail: wwardhana@ugm.ac.id

Article Info
https://doi.org/10.31018/jans.v15i3.4781
Received: June 5, 2023
Revised: August 21, 2023
Accepted: August 25, 2023

How to Cite
Umarhadi, D. A. *et al.* (2023). Monitoring forest gain and loss based on LandTrendr algorithm and Landsat images in KTH Pati social forestry area, Indonesia. *Journal of Applied and Natural Science*, 15(3), 1051 - 1060. https://doi.org/10.31018/jans.v15i3.4781

Abstract
Social forestry schemes are now being implemented in numerous state forest areas in Indonesia, aiming to reduce deforestation and improve the community's livelihood. However, spatial monitoring in the social forestry area is still limited to see how the implementation progresses. The present study aimed to identify the change of forest taking a case in Pati Forest Farmer Communities (KTH Pati) social forestry area from 1996 to 2022 using the LandTrendr algorithm based on Normalized Burn Ratio (NBR) value of Landsat image series. The results detected forest loss and gain covering an area of 453.97 ha and 494.18 ha, respectively. Two main reasons causing the forest loss are the country's financial and political situation from 1997 to 2003 and the harvest of forest plantations in 2017–2018. However, it was found that the study area had a positive forest gain with the current continuous growth of 292.32 ha (20.16% of the total area). Even though the social forestry policy has not significantly shown a positive impact on forest growth, spatial monitoring through remote sensing can be a great tool for observing the progress.

Keywords: Forest change, NBR, Remote sensing, Satellite imagery, Spectral trajectory

INTRODUCTION

The decrease in forest area has occurred globally in the last decades, with a loss of 178 Mha between 1990 and 2020, leaving to cover 31% (4.06 billion ha) of the total land area (Sarre, 2020). Tropical forests are the vastest among other regions, accounting for 45% of the global forest area and contributing to 200–300 Pg C from its living trees, equivalent to one-third of carbon in the atmosphere (Mitchard, 2018; Sarre, 2020). Reducing the deforestation rate of tropical forests is essential to mitigate climate change and preserve worldwide biodiversity (Buizer *et al.*, 2014; Gullison *et al.*, 2007; Strassburg *et al.*, 2012). On the other hand, developing countries, including Indonesia, still rely on forests for economic growth and to meet the people's needs from the forests (Nerfa *et al.*, 2020; Sunderlin *et al.*, 2005). These circumstances lead to the emergence of community-based forestry, allowing the local community to manage and utilize forest resources to improve their lives without neglecting the sustainability of forests themselves (Gilmour, 2016).

In Indonesia, social forestry, also known as community-based forestry, is defined as a sustainable forest management system in the State or privately-owned forest areas implemented by local or indigenous communities as the main actors to improve their welfare, environmental balance, and socio-cultural dynamics (Ministry of Environment and Forestry, 2021). This system can be in the form of village forest, community forest, forest community crop, *Adat* (customary) forest, and forestry partnerships. Through social forestry, communities have legal access to utilize the State's forest area for timber and non-timber plantations (Ministry of Environment and Forestry, 2022).

Considering the importance of social forestry for economic growth and the sustainability of forests, the Indonesian government has targeted to increase the area of social forestry to 12.7 Mha by 2021 (Maryudi, 2017; Rakatama and Pandit, 2020). As of October 2022, 5.1 Mha, or about 4.7% of the state's forest area has been legalized for social forestry (Directorate General of Social Forestry and Environmental Partnerships, 2022).

Reportedly, the deforestation rate declined in the forest under the village forest scheme of social forestry in Kalimantan and Sumatera, Indonesia, even though biophysical and anthropogenic factors influence the performances and differ in terms of time and space (Santika *et al.*, 2017). Social forestry under the community forest scheme also led to the reduction of forest cover loss in Lampung province, although the deforestation rate was below the designated conservation and protection forests (Putraditama *et al.*, 2019).

Using remote sensing data, Sadono *et al.* (2020) found that community involvement in social forestry could even help restore tree coverage through a rehabilitation activity included. The forest condition was monitored through multi-temporal Landsat images with a temporal gap between 4–9 years (Sadono *et al.*, 2020). The availability of Landsat images since the seventies allows dense time-series analysis over a certain area (Umarhadi *et al.*, 2022). The dynamic change of vegetation can be monitored by observing the spectral trajectory of an individual pixel over time (Yang *et al.*, 2018). Taking advantage of prolonged Landsat data acquisition, Kennedy *et al.* (2010) have developed LandTrendr (Landsat-based detection of Trends in Disturbance and Recovery) that creates line segments to obtain spectral trajectories of objects based on annual image observation. LandTrendr can detect forest change, both gain and loss, with the attributes consisting of the change time, magnitude, and duration. This algorithm has been widely applied to various cases, including mining activity (Dlamini and Xulu, 2019; Sari *et al.*, 2022; Xiao *et al.*, 2020; Yang *et al.*, 2018), wetlands (de Jong *et al.*, 2021; Fu *et al.*, 2022; Sari *et al.*, 2022), croplands (Zhu *et al.*, 2019), and general forest monitoring (Shen *et al.*, 2022; Yin *et al.*, 2022).

This study aimed to identify the trends of forest change using the LandTrendr approach, taking a case study in a social forestry area in Pati, Indonesia. Further, it was intended to understand the dynamic change of forests where local communities are primarily involved in the management.

MATERIALS AND METHODS

Study area

The study area is located in a social forestry area of Pati consisting of two Forest Farmer Communities (*Kelompok Tani Hutan* [KTH]), i.e., KTH Sukobubuk Rejo and KTH Patiayam Rejo. The two KTH areas in the remainder of this article are called KTH Pati social forestry area. The Ministry of Environment and Forestry designated this area as a production and limited-production forest. The permission for the social forestry area is regulated by the decree of the Minister of Environment and Forestry through (SK. 4967/MENLHK-PSKL/PKPS/PSL.0/7/2018), which was issued on 27th July 2018 (Ministry of Environment and Forestry, 2019). Before that, the intercropping practice was implemented earlier, followed by community-based forest management (Widjayanti, 1989). In the study area, community-based forest management was initiated in 2002 by establishing a forest village community institution that cooperates with Perum Perhutani who is the authority to manage the area (Pranoto, 2020).

KTH Pati social forestry area covers 1,934 ha, including 1,464 households within the area. The present study used an indicative area that the management unit had categorized. It covers an area of 1,450 ha, situated within the geographic coordinates of 6°43'59"–6°46'45" S and 110°56'4"–110°59'2" E as shown in Fig. 1. A variety of plants were cultivated by the community including Sengon (*Albizia chinensis*), Balsa (*Ochroma pyramidale*), Mango (*Mangifera indica*), Avocado (*Persea americana*), Petai (*Parkia speciosa*), Ambarella (*Spondias dulcis*), and Jackfruit (*Artocarpus heterophyllus*).

Image collection and pre-processing

Multispectral Landsat imageries from the launch of Thematic Mapper (TM) to Operational Land Imager (OLI) provide the longest series of earth observations since the 1980s with a consistent spatial resolution at 30 m and comparable spectral specifications (Wulder *et al.*, 2022). The Landsat archive data are made publicly accessible on Google Earth Engine (GEE) in which data acquisition, pre-processing, and main LandTrendr processing were performed in this study (Kennedy *et al.*, 2018).

This study used Landsat 5 TM, Landsat 7 ETM+ (Enhanced Thematic Mapper Plus), Landsat 8 OLI, and Landsat 9 OLI with an observation period between 1996 and 2022. Image filter was applied to only include images acquired within June–September to diminish seasonal vegetation change. All images are in Level 2 surface reflectance after being processed with the Landsat Ecosystem Disturbance Adaptive Processing System (LEDAPS) algorithm for Landsat 5–7 and the Land Surface Reflectance Code (LaSRC) algorithm for

Table 1. Defined segmentation parameters for LandTrendr algorithm

Parameter	Value
Maximum segmentations	6
Spike threshold	0.9
Vertex count overshoot	3
Prevent one-year recovery	True
Recovery threshold	0.25
p-value threshold	0.05
Best model proportion	0.75
Minimum observations needed	6

Landsat 8–9 (Schmidt *et al.*, 2013; Vermote *et al.*, 2016). Sensor-to-sensor harmonization was performed using the equations by Roy et al., (2016) to minimise the spectral differences. The medoid filtering technique was used to generate the most representative pixel in a year composite by choosing the pixel value having the smallest sum of squared differences between the median values of a certain band and across bands (de Jong *et al.*, 2021).

We then transformed the pixels to Normalized Burn Ratio (NBR) to construct the pixel-level of time-series observation. The bands used in NBR, i.e., short-wave infrared 2 and near-infrared, have a strong complementary power for forest disturbance detection, making this index sensitive to forest disturbance (Cohen *et al.*, 2018). NBR is classified as a ratio index, thus it can minimize the spectral noises from the local topography (Umarhadi and Danoedoro, 2020). The NBR equation is as follows (García and Caselles, 1991):

$$NBR = (NIR - SWIR2) / (NIR + SWIR2) \qquad \text{Eq. 1}$$

where NIR denotes the near-infrared band and SWIR2 denotes the short-wave infrared band of the corresponding pixel. The images of NBR index are shown in Fig. 2.

LandTrendr processing

This study applied LandTrendr algorithm implemented on Google Earth Engine, referring to Kennedy *et al.* (2018). LandTrendr algorithm employs a temporal segmentation method on the values of the derived vegetation index that will generate the information on vegetation loss and gain of the forest. LandTrendr algorithm comprises six stages, i.e., 1) noise-induced spikes removal (residual clouds, snow, smoke, or shadows), 2) potential vertices identification using regression approach, 3) trajectories fitting, 4) model simplification, 5) the best model determination based on the p-value for the F-statistic, and 6) segmentation results evaluation (Kennedy *et al.*, 2010). The parameters used for the processing are presented in Table 1.

Both forest loss and gain were generated separately. For this study, we selected the greatest change scenario. Thus, the final results represent the biggest disturbance within the observation period. A magnitude filtering was applied to consider the changes in NBR value more than 0.1. The changes in an area of about a half hectare (0.54 ha) or 6 pixels of Landsat image were taken into account for the minimum mapping unit. The processing results were the duration, magnitude, and occurrence year of vegetation loss and gain. Fig. 3 depicts the illustration of temporal segment attributes in the case of forest loss indicated by the decline of spectral value. In contrast, forest gain was determined by the increase in spectral value in the following year(s).

Validation

An accuracy assessment was conducted to evaluate the LandTrendr results by validating the year of change using the temporal segmentation and visual image interpretation of Landsat images and Google Satellite

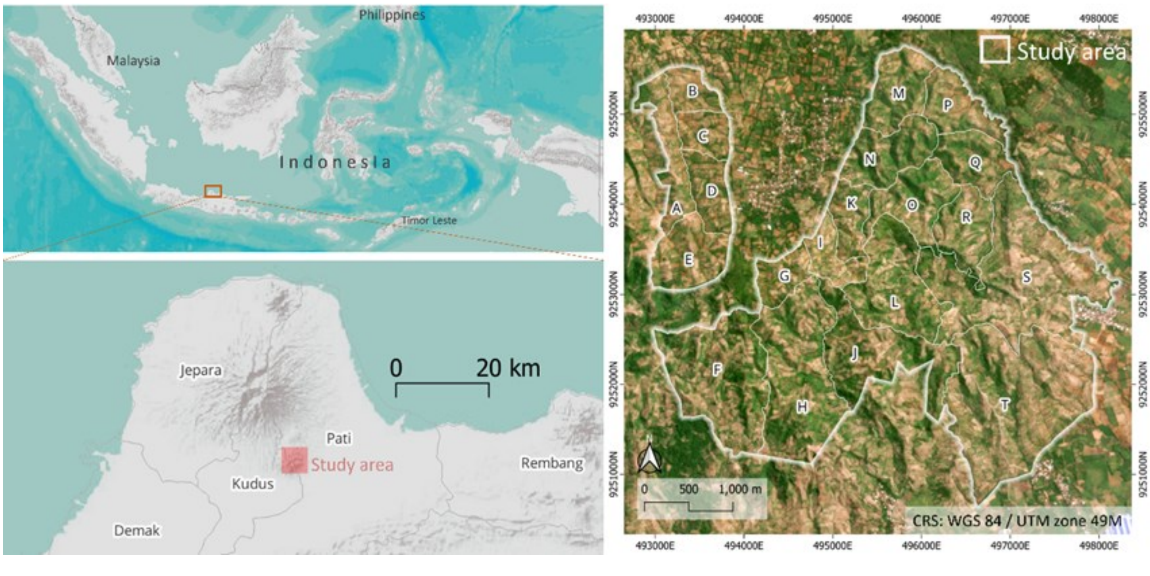

Fig. 1. *Study area located in KTH Pati social forestry area, Indonesia; Alphabetical block unit is assigned to simplify the actual name for the analysis*

Table 2. Area and magnitude average per block unit in KTH Pati social forestry area

Block	Loss		Gain	
	Area (ha)	**Magnitude average**	**Area (ha)**	**Magnitude average**
A	8.33	320	15.48	237
B	0.06	585	9.80	188
C	0.92	354	7.63	210
D	13.17	407	24.18	340
E	4.65	290	5.66	216
F	55.34	310	30.00	250
G	2.12	312	7.06	192
H	57.56	344	38.79	256
I	1.65	136	3.20	201
J	40.82	299	27.54	268
K	3.85	198	7.64	171
L	41.75	377	39.91	225
M	3.05	258	28.33	204
N	6.17	219	34.87	229
O	4.90	289	18.20	193
P	5.70	405	22.51	278
Q	18.38	364	16.19	217
R	9.43	267	8.48	183
S	107.65	344	69.52	224
T	68.47	326	79.19	281

images where available. We used TimeSync tools to clip the corresponding sample area and display the trajectory of NBR throughout the observation period (Cohen *et al.*, 2010). A total of 150 sample points were stratified-randomly selected: every 75 samples for vegetation loss and gain, respectively. Confusion matrices were then created to quantify the accuracy of the maps.

RESULTS AND DISCUSSION

Area of forest change

LandTrendr algorithm resulted in three main results consisting of duration, magnitude, and year of change on loss and gain, respectively (Fig. 4). As shown in the maps and Table 2, in total, we identified forest loss covering an area of 453.97 ha, while the forest gain covered 494.18 ha. The greatest area encountered loss is in Block S, with an area of 107.65 ha or about half (53%) of the block area. It was followed by Blocks T (68.47 ha), H (57.56 ha), F (55.34 ha), L (41.75 ha), and J (40.82 ha). Based on the loss magnitude, Blocks B, D, and P exhibit the highest average loss magnitude, i.e., 585, 407, and 405, respectively. However, the loss in Block B only covered quite a small area (0.06 ha).

Similar to the loss, the two blocks of the vastest vegetation gain area occurred in Blocks T (79.19 ha) and S (69.52 ha). The vegetation gain is more distributed over the whole study area compared to the loss with the least area in Block I (3.20 ha). Nevertheless, the mean gain magnitudes in all blocks ranged between 171 and 256, except for Block D, which reached 340. Block D managed to have the highest percentage of the gain area (69.62%), followed by Blocks N (63.11%), M (56.61%), and P (54.17%).

Time scale of forest change

Fig. 5 depicts the extent of forest change in terms of time. More than half of vegetation loss and gain occurred in 1997, with a percentage of 51.48% (234.45 ha) and 61.84% (61.84 ha) of the total loss and gain, respectively. Since the beginning of our observation period, the forest change might be affected by the economic crisis 1997 in Indonesia, causing intensive logging in the study area. It can be seen in Fig. 6 that the loss magnitude in 1997 was relatively higher. Conversely, although the area of gain is also broad in 1997, the magnitude is not above average.

In 1998, at the beginning of the reformation era after the fall of the Soeharto political regime, forests were generally directly benefited by the communities; thus encroachment inside the forest area was inevitable (Nawir and Rumboko, 2007). The present results proved that a forest area of 172.80 ha was deforested during 1999–2003 (Fig. 5). From 2004 to 2016, the changes were relatively stable. The most recent forest loss was identified in 2017–2018 with a loss of 31.95 ha. As shown in Fig. 4, most losses occurred in Block D. This block was intended for the forest plantations by the authority. Therefore, it showed a positive trend from 1997, yet after around 20 years, the plantations were harvested.

As observed in Fig. 6, the duration of loss was generally shorter than the gain, with an average of 7.44 years compared to 19.18 years. This shows that overall, the

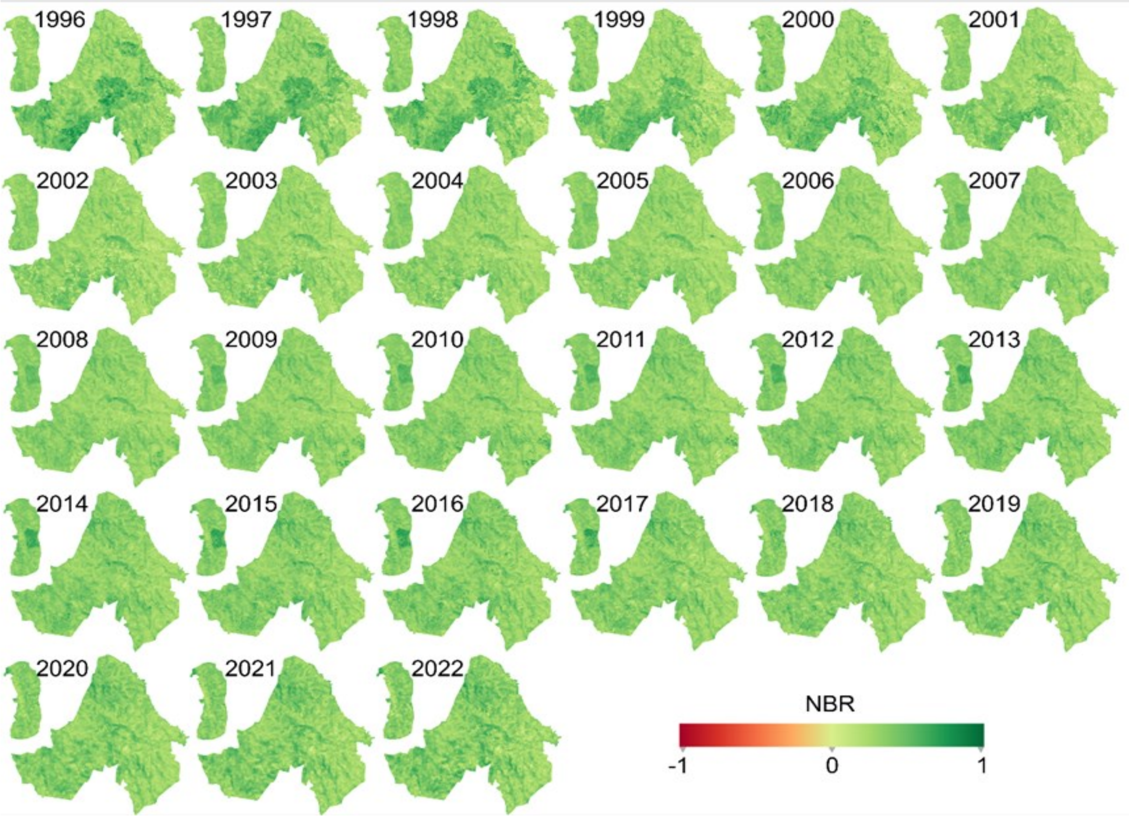

Fig. 2. *Normalized Burn Ratio (NBR) images from 1996 to 2022 for LandTrendr processing*

recovery takes 7.44 years after loss occurred in the study area. More than half of the gain (58.82%) was ongoing at the end of the observation period in 2022. Although the mean gain magnitude was quite low, i.e., 230, the trend proved that an area of 292.32 ha showed continuous forest growth. Notably, there was no new forest gain between 2014 and 2017, yet the loss occurred in an area of 28 ha within those years. It might be due to the transition before the social forestry permit was granted.

Trade-off between forest gain and loss

By overlaying the area of loss and gain, we generated the area interchanged between gain and loss. As shown in Fig. 7a, the gain in the deforested areas previously occurred mainly from 2000 to 2003. This indicated although massive deforestation occurred in this period, as discussed earlier, the community might also contribute to the revegetation of the deforested area through the scheme of community-based forest management. Fig. 7b shows that the firstly gained forest experienced loss in 1999–2002. This graph also displays that the forest area which had been growing detected from the beginning of the observation period in Block D experienced a loss in 2017–2018.

Impact of social forestry and its role in forest change

Based on the timeline, the local community implemented the intercropping practice, and then community-based forest management was established in 2002 under the authority of Perum Perhutani. The locals were permitted to plant and utilize forest products in the forest area with a maximum of 25% profit sharing for the community (Yokota et al., 2014). With the issuance of ministerial regulation regarding social forestry, the community has been fully granted to manage the forest area since 2018. This scheme is more beneficial for the community due to the greater profit sharing for the community, referring to the Regulation of The Minister of Environment and Forestry No. 39 of the Year 2017. Pranoto (2020) reported that the people's annual income increased to 22% after social forestry was

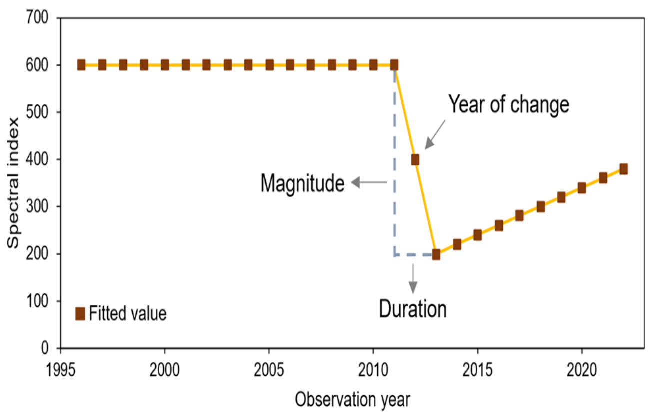

Fig. 3. *Temporal segmentation showing the attributes of LandTrendr algorithm.*

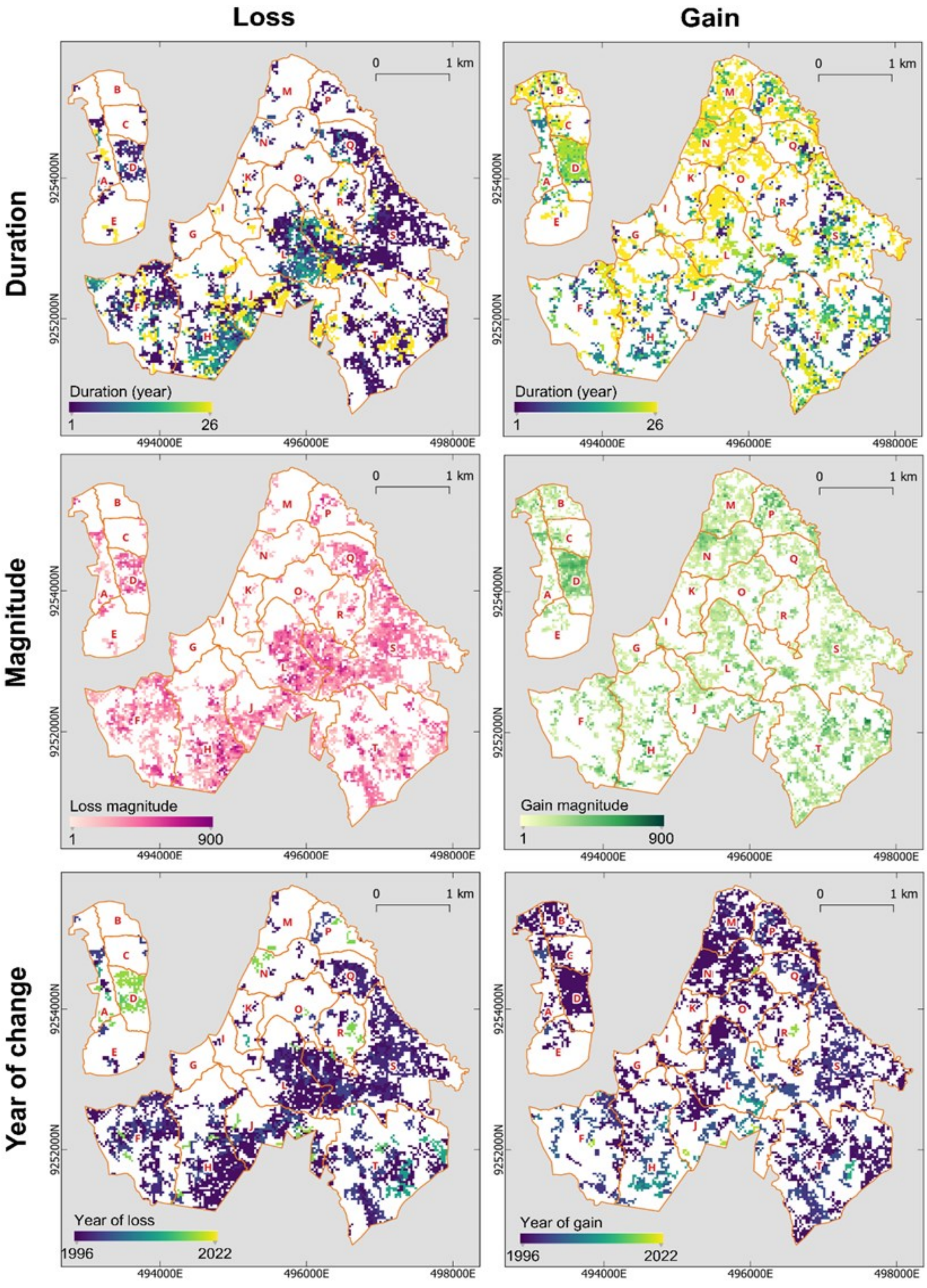

Fig. 4. *Results of LandTrendr algorithm including duration, magnitude, and year of change of forest loss and gain. Note that the resulted magnitude is multiplied by 1,000*

implemented in KTH Pati.

As part of the social forestry scheme, the local community must maintain forest function by planting forest trees besides multipurpose trees and crops. The present study found that forest change can be suppressed by implementing community-based forest management (2002–2018), as also stated by Fujiwara *et al.* (2012). The remaining stable forest change continued as social forestry was granted in 2018 (Fig. 5). Although a positive forest gain was identified through our analysis, the implementation of social forestry has not significantly increased the forest coverage in the area. This is mainly

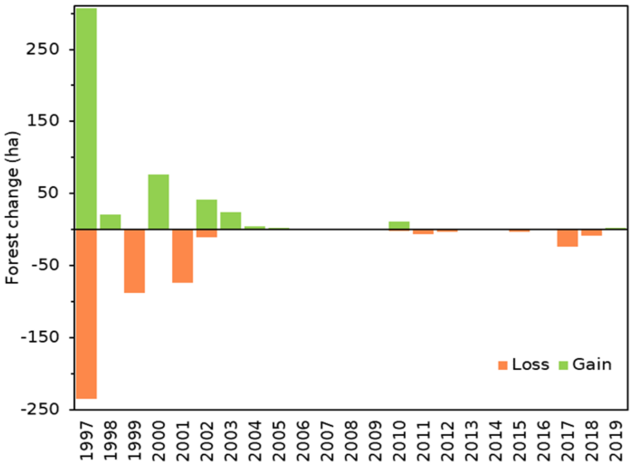

Fig. 5. *Total area of forest loss and gain in KTH Pati social forestry area with respect to the time*

because most forest farmers still prioritized crops such as corn and cassava as their primary commodity since forest and multipurpose trees take time to be harvested (Pranoto, 2020). Therefore, it is noteworthy that the forest area should be spatially monitored in the upcoming years.

Validation and method evaluation

A total of 150 sample points of vegetation loss and gain were validated by analyzing the NBR trajectories generated from LandTrendr processing and visually interpreting Landsat images and high-resolution Google Satellite images. Observing the imageries can detect the occurrence year to validate whether the sample points are experiencing the change at the correct time. Figs. 8a and 8b show the forest loss and gain confusion

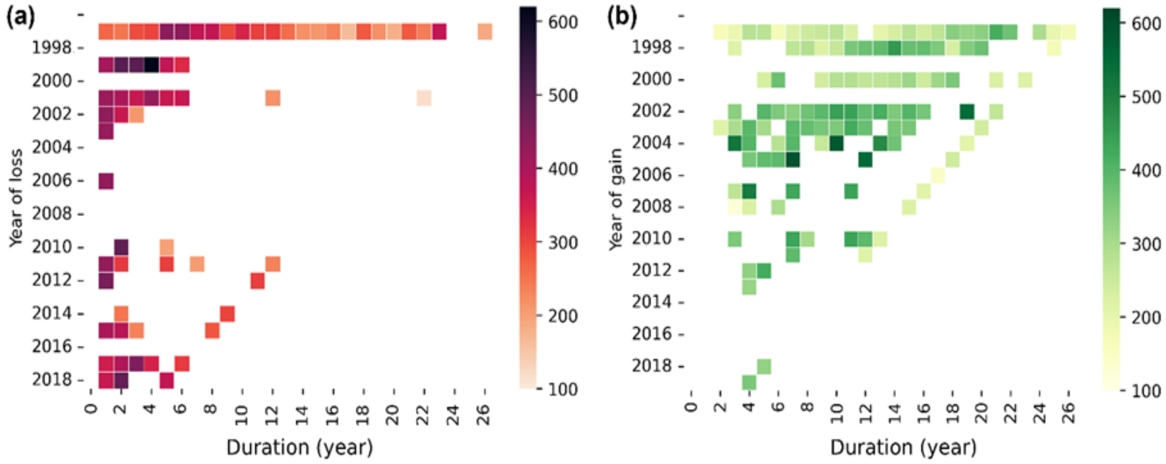

Fig. 6. *Total area of (a) forest loss and (b) gain in the matrix of occurrence year and duration*

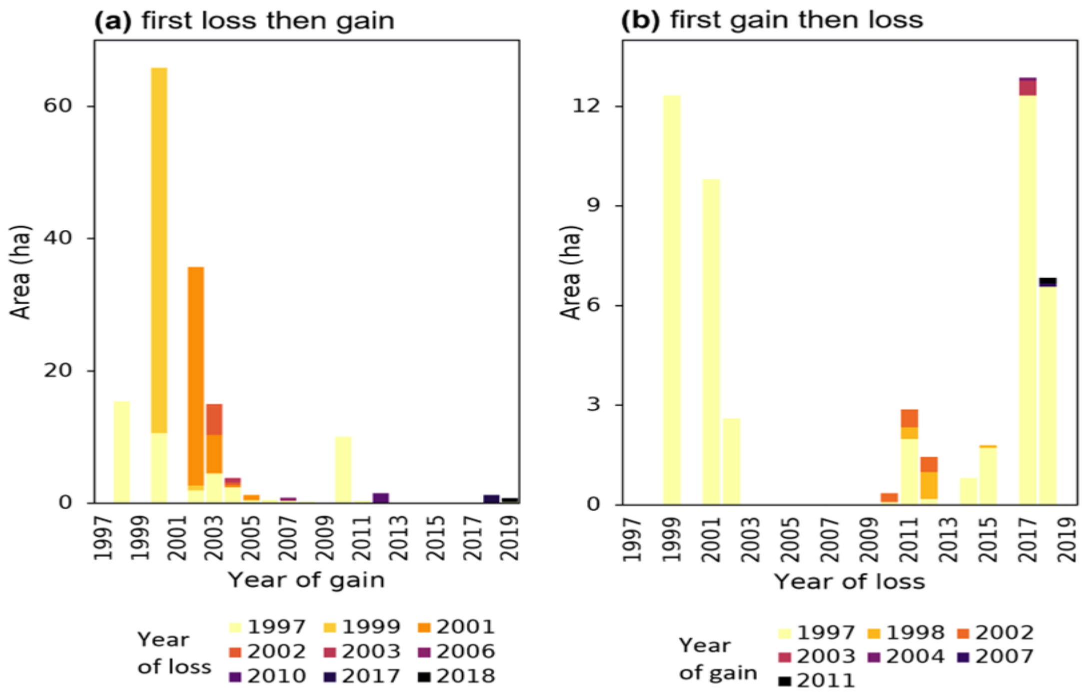

Fig. 7. *Total area of forests experiencing (a) a forest gain after loss and (b) a loss after gain*

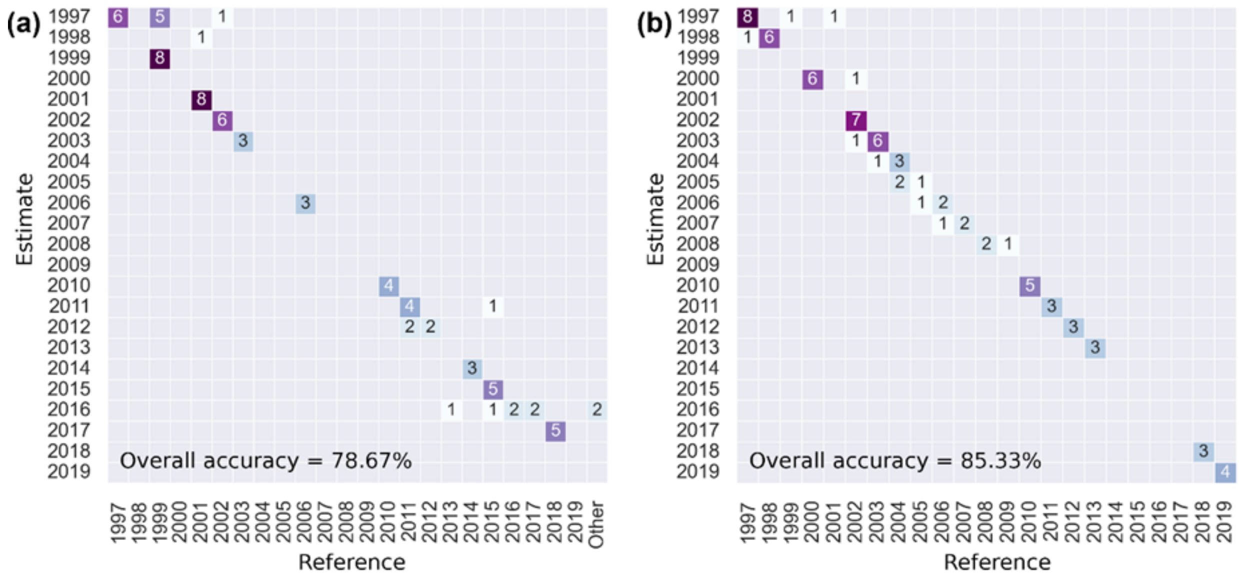

Fig. 8. *Confusion matrices showing the accuracy of (a) forest loss and (b) gain resulted from LandTrendr algorithm*

matrices, respectively. Vegetation loss exhibits an overall accuracy of 78.67% which is lower than the gain (85.33%). The high inaccuracy in forest loss is shown in 1997, with 6 points incorrectly classified. This error is mainly because the p-value threshold of the regression (0.05) was not reached by the fitted trajectory, leading to the simplified straight lines for a long period starting from the beginning of the observation time (Yang *et al.*, 2018). However, overall, the forest gain and loss estimates have met decent accuracy.

The present study applied LandTrendr algorithm using Landsat archive images, taking advantage of the prolonged observation period. However, the medium resolution (30 m) provided by Landsat images may not detect small disturbances, instead of generalisation of the given pixel size (Fu et al., 2022). The Pan-sharpening method can be employed to increase the Landsat resolution to 15 m using a panchromatic band. Nevertheless, this method can only be applied for the observation after 1999 since the panchromatic band is available in Landsat 7 ETM+ and Landsat 8–9 OLI (Amini et al., 2022). Sentinel-2 is the alternative offering higher spatial resolution (10 m for visible and near-infrared bands) with dense temporal resolution (up to 5 days). However, as the first observation of Sentinel-2 started in 2015, it limits the observation period to less than 10 years (Yin et al., 2022). Future studies can consider the employment of higher spatial resolution either derived from the pan-sharpening method or the use of Sentinel-2 images in LandTrendr algorithm.

Our trend analysis using LandTrendr algorithm can be utilized to continuously monitor social forestry's progress. This study used the most significant change scenario by neglecting the lower magnitude changes. The lower rate changes might also happen in the past several years in the study area. Therefore, future studies should consider involving more minor changes for the analysis.

Conclusion

This study demonstrates the trend identification of forest loss and gain in KTH Pati social forestry area using time-series Landsat images during 1996–2022 based on the LandTrendr algorithm. By applying the greatest change scenario, we found that the forest gain is vaster, with an area of 494.18 ha, compared to forest loss (453.97 ha). The financial and political situation at the beginning of our observation period affected the forest condition as we observed an immense loss in 1997, followed by a loss in 1999–2003. This study detected a positive forest gain, as shown by the continuous forest growth on an area of 292.32 ha or 58.82% of the total gain area. The interchanged area was also detected by combining the loss and gain scenarios. This analysis displayed that the recovery in the formerly deforested areas mainly occurred during 2000–2003. On the other hand, the harvest of forest plantations was also detected in 2017–2018 on Block D. This indicated that the community has a role in managing social forestry areas. Although the impact of the social forestry scheme on the forest gain is yet to show a significant result, the progress can be monitored through remote sensing technology with LandTrendr method.

ACKNOWLEDGEMENTS

We thank the editor and reviewers for their valuable comments and suggestions.

Conflict of interest

The authors declare that they have no conflict of interest.

REFERENCES

1. Amini, S., Saber, M., Rabiei-Dastjerdi, H. & Homayouni, S. (2022). Urban Land Use and Land Cover Change Analysis Using Random Forest Classification of Landsat Time Series. *Remote Sensing*, *14*(11), 2654. https://doi.org/10.3390/rs14112654
2. Buizer, M., Humphreys, D. & de Jong, W. (2014). Climate change and deforestation: The evolution of an intersecting policy domain. *Environmental Science & Policy*, *35*, 1–11. https://doi.org/10.1016/j.envsci.2013.06.001
3. Cohen, W. B., Yang, Z., Healey, S. P., Kennedy, R. E. & Gorelick, N. (2018). A LandTrendr multispectral ensemble for forest disturbance detection. *Remote Sensing of Environment*, *205*, 131–140. https://doi.org/10.1016/j.rse.2017.11.015
4. Cohen, W. B., Yang, Z. & Kennedy, R. (2010). Detecting trends in forest disturbance and recovery using yearly Landsat time series: 2. TimeSync — Tools for calibration and validation. *Remote Sensing of Environment*, *114*(12), 2911–2924. https://doi.org/10.1016/j.rse.2010.07.010
5. de Jong, S. M., Shen, Y., de Vries, J., Bijnaar, G., van Maanen, B., Augustinus, P. & Verweij, P. (2021). Mapping mangrove dynamics and colonization patterns at the Suriname coast using historic satellite data and the LandTrendr algorithm. *International Journal of Applied Earth Observation and Geoinformation*, *97*, 102293. https://doi.org/10.1016/j.jag.2020.102293
6. Directorate General of Social Forestry and Environmental Partnerships. (2022, October 3). *Capaian Perhutanan Sosial Sampai Dengan 1 Oktober 2022*. http://pskl.menlhk.go.id/berita/437-capaian-perhutanan-sosial-sampai-dengan-1-oktober-2022.html?showall=&limitstart=
7. Dlamini, L. Z. D. & Xulu, S. (2019). Monitoring Mining Disturbance and Restoration over RBM Site in South Africa Using LandTrendr Algorithm and Landsat Data. *Sustainability*, *11*(24), 6916. https://doi.org/10.3390/su11246916
8. Fu, B., Lan, F., Xie, S., Liu, M., He, H., Li, Y., Liu, L., Huang, L., Fan, D., Gao, E. & Chen, Z. (2022). Spatio-temporal coupling coordination analysis between marsh vegetation and hydrology change from 1985 to 2019 using LandTrendr algorithm and Google Earth Engine. *Ecological Indicators*, *137*, 108763. https://doi.org/10.1016/j.ecolind.2022.108763
9. Fujiwara, T., Septiana, R. M., Awang, S. A., Widayanti, W. T., Bariatul, H., Hyakumura, K. & Sato, N. (2012). Changes in local social economy and forest management through the introduction of collaborative forest management (PHBM), and the challenges it poses on equitable partnership: A case study of KPH Pemalang, Central Java, Indonesia. *Tropics*, *20*(4), 115–134. https://doi.org/10.3759/tropics.20.115
10. García, M. J. L. & Caselles, V. (1991). Mapping burns and natural reforestation using thematic Mapper data. *Geocarto International*, *6*(1), 31–37. https://doi.org/10.1080/10106049109354290
11. Gilmour, D. A. (2016). *Forty years of community-based forestry: A review of its extent and effectiveness*. Food and agriculture organization of the United Nations.
12. Gullison, R. E., Frumhoff, P. C., Canadell, J. G., Field, C. B., Nepstad, D. C., Hayhoe, K., Avissar, R., Curran, L. M., Friedlingstein, P., Jones, C. D. & Nobre, C. (2007). Tropical Forests and Climate Policy. *Science*, *316*(5827), 985–986. https://doi.org/10.1126/science.1136163
13. Kennedy, R. E., Yang, Z. & Cohen, W. B. (2010). Detecting trends in forest disturbance and recovery using yearly Landsat time series: 1. LandTrendr — Temporal segmentation algorithms. *Remote Sensing of Environment*, *114* (12), 2897–2910. https://doi.org/10.1016/j.rse.2010.07.008
14. Kennedy, R. E., Yang, Z., Gorelick, N., Braaten, J., Cavalcante, L., Cohen, W. & Healey, S. (2018). Implementation of the LandTrendr Algorithm on Google Earth Engine. *Remote Sensing*, *10*(5), 691. https://doi.org/10.3390/rs10050691
15. Maryudi, A. (2017). Creating New Forest Governance Structure for the 12.7 Million-Promise. *Jurnal Ilmu Kehutanan*, *11*(1), 1–3.
16. Ministry of Environment and Forestry. (2019). *Statistik Lingkungan Hidup dan Kehutanan Tahun 2018*. Pusat Data dan Informasi KLHK.
17. Ministry of Environment and Forestry. (2021). *Peraturan Menteri Lingkungan Hidup dan Kehutanan tentang Pengelolaan Perhutanan Sosial (Ministerial Regulation on the Social Forestry Management) No. 9 Year 2021*. Ministry of Environment and Forestry Republic of Indonesia.
18. Ministry of Environment and Forestry. (2022). *The State of Indonesia's Forests 2022*. Ministry of Environment and Forestry, Republic of Indonesia.
19. Mitchard, E. T. A. (2018). The tropical forest carbon cycle and climate change. *Nature*, *559*(7715), 527–534. https://doi.org/10.1038/s41586-018-0300-2
20. Nawir, A. A. & Rumboko, L. (2007). History and State of Deforestation and Land Degradation. In A. A. Nawir, Murniati, & L. Rumboko (Eds.), *Forest rehabilitation in Indonesia: Where to after more than three decades?* (pp. 11–32). Center for International Forestry Research.
21. Nerfa, L., Rhemtulla, J. M. & Zerriffi, H. (2020). Forest dependence is more than forest income: Development of a new index of forest product collection and livelihood resources. *World Development*, *125*, 104689. https://doi.org/10.1016/j.worlddev.2019.104689
22. Pranoto, D. V. (2020). *Analysis of Diversity Sources and Amount of Household Income and Their Inequalities in IPHPS Holder Farmers in Sukobubuk Village, Pati District* [Undergraduate Thesis]. Universitas Gadjah Mada.
23. Putraditama, A., Kim, Y.-S. & Sánchez Meador, A. J. (2019). Community forest management and forest cover change in Lampung, Indonesia. *Forest Policy and Economics*, *106*, 101976. https://doi.org/10.1016/j.forpol.2019.101976
24. Rakatama, A. & Pandit, R. (2020). Reviewing social forestry schemes in Indonesia: Opportunities and challenges. *Forest Policy and Economics*, *111*, 102052. https://doi.org/10.1016/j.forpol.2019.102052
25. Sadono, R., Pujiono, E. & Lestari, L. (2020). Land cover changes and carbon storage before and after community forestry program in Bleberan village, Gunungkidul, Indonesia, 1999–2018. *Forest Science and Technology*, *16*(3), 134–144. https://doi.org/10.1080/21580103.2020.1801523
26. Santika, T., Meijaard, E., Budiharta, S., Law, E. A., Kusworo, A., Hutabarat, J. A., Indrawan, T. P., Struebig, M., Raharjo, S., Huda, I., Sulhani, Ekaputri, A. D., Trison, S.,

Stigner, M. & Wilson, K. A. (2017). Community forest management in Indonesia: Avoided deforestation in the context of anthropogenic and climate complexities. *Global Environmental Change*, *46*, 60–71. https://doi.org/10.1016/j.gloenvcha.2017.08.002

27. Sari, S. P., Feyen, J., Koedam, N. & Van Coillie, F. (2022). Monitoring Trends of Mangrove Disturbance at the Tin Mining Area of Bangka Island Using Landsat Time Series and Landtrendr. *IGARSS 2022 - 2022 IEEE International Geoscience and Remote Sensing Symposium*, 457–460. https://doi.org/10.1109/IGARSS46834.2022.9883322
28. Sarre, A. (Ed.). (2020). *Global forest resources assessment, 2020: Main report*. Food and Agriculture Organization of the United Nations.
29. Schmidt, G. L., Jenkerson, C. B., Masek, J., Vermote, E. & Gao, F. (2013). *Landsat ecosystem disturbance adaptive processing system (LEDAPS) algorithm description* (U.S. Geological Survey Open-File Report 2013–1057; p. 17). U.S. Geological Survey.
30. Shen, J., Chen, G., Hua, J., Huang, S. & Ma, J. (2022). Contrasting Forest Loss and Gain Patterns in Subtropical China Detected Using an Integrated LandTrendr and Machine-Learning Method. *Remote Sensing*, *14*(13), 3238. https://doi.org/10.3390/rs14133238
31. Strassburg, B. B. N., Rodrigues, A. S. L., Gusti, M., Balmford, A., Fritz, S., Obersteiner, M., Kerry Turner, R. & Brooks, T. M. (2012). Impacts of incentives to reduce emissions from deforestation on global species extinctions. *Nature Climate Change*, *2*(5), 350–355. https://doi.org/10.1038/nclimate1375
32. Sunderlin, W. D., Angelsen, A., Belcher, B., Burgers, P., Nasi, R., Santoso, L. & Wunder, S. (2005). Livelihoods, forests, and conservation in developing countries: An Overview. *World Development*, *33*(9), 1383–1402. https://doi.org/10.1016/j.worlddev.2004.10.004
33. Umarhadi, D. A. & Danoedoro, P. (2020). The Effect of Topographic Correction on Canopy Density Mapping Using Satellite Imagery in Mountainous Area. *International Journal on Advanced Science, Engineering and Information Technology*, *10*(3), 1317. https://doi.org/10.18517/ijaseit.10.3.7739
34. Umarhadi, D. A., Widyatmanti, W., Kumar, P., Yunus, A. P., Khedher, K. M., Kharrazi, A. & Avtar, R. (2022). Tropical peat subsidence rates are related to decadal LULC changes: Insights from InSAR analysis. *Science of The Total Environment*, *816*, 151561. https://doi.org/10.1016/j.scitotenv.2021.151561
35. Vermote, E., Justice, C., Claverie, M. & Franch, B. (2016). Preliminary analysis of the performance of the Landsat 8/OLI land surface reflectance product. *Remote Sensing of Environment*, *185*, 46–56. https://doi.org/10.1016/j.rse.2016.04.008
36. Widjayanti, R. R. D. (1989). *Dinamika Kelompok Tani Hutan dalam Program Perhutanan Sosial (Social Forestry) Studi Kasus di Desa Sukobubuk Pati, Jawa Timur*.
37. Wulder, M. A., Roy, D. P., Radeloff, V. C., Loveland, T. R., Anderson, M. C., Johnson, D. M., Healey, S., Zhu, Z., Scambos, T. A., Pahlevan, N., Hansen, M., Gorelick, N., Crawford, C. J., Masek, J. G., Hermosilla, T., White, J. C., Belward, A. S., Schaaf, C., Woodcock, C. E., … Cook, B. D. (2022). Fifty years of Landsat science and impacts. *Remote Sensing of Environment*, *280*, 113195. https://doi.org/10.1016/j.rse.2022.113195
38. Xiao, W., Deng, X., He, T. & Chen, W. (2020). Mapping Annual Land Disturbance and Reclamation in a Surface Coal Mining Region Using Google Earth Engine and the LandTrendr Algorithm: A Case Study of the Shengli Coalfield in Inner Mongolia, China. *Remote Sensing*, *12*(10), 1612. https://doi.org/10.3390/rs12101612
39. Yang, Y., Erskine, P. D., Lechner, A. M., Mulligan, D., Zhang, S. & Wang, Z. (2018). Detecting the dynamics of vegetation disturbance and recovery in surface mining area via Landsat imagery and LandTrendr algorithm. *Journal of Cleaner Production*, *178*, 353–362. https://doi.org/10.1016/j.jclepro.2018.01.050
40. Yin, X., Kou, W., Yun, T., Gu, X., Lai, H., Chen, Y., Wu, Z. & Chen, B. (2022). Tropical Forest Disturbance Monitoring Based on Multi-Source Time Series Satellite Images and the LandTrendr Algorithm. *Forests*, *13*(12), 2038. https://doi.org/10.3390/f13122038
41. Yokota, Y., Harada, K., Rohman, Silvi, N. O., Wiyono, Tanaka, M. & Inoue, M. (2014). Contributions of Company-Community Forestry Partnerships (PHBM) to the Livelihoods of Participants in Java, Indonesia: A Case Study in Madiun, East Java. *Japan Agricultural Research Quarterly: JARQ*, *48*(3), 363–377. https://doi.org/10.6090/jarq.48.363
42. Zhu, L., Liu, X., Wu, L., Tang, Y. & Meng, Y. (2019). Long-Term Monitoring of Cropland Change near Dongting Lake, China, Using the LandTrendr Algorithm with Landsat Imagery. *Remote Sensing*, *11*(10), 1234. https://doi.org/10.3390/rs11101234